Covert ISAC: Towards Collusive Detection

Yujie Wu[†], Chengwen Xing[§], Jie Tang[‡], Nan Zhao[†], Xiu Yin Zhang[‡], Kai-Kit Wong^{*}, George K. Karagiannidis^{*}

†School of Information and Communication Engineering, Dalian University of Technology, Dalian 116024, China

§School of Information and Electronics, Beijing Institute of Technology, Beijing 100081, P. R. China

†School of Electronic and Information Engineering, South China University of Technology, Guangzhou 510641, China

*Department of Electronic and Electrical Engineering, University College London, London WC1E 6BT, United Kingdom

*Department of Electrical and Computer Engineering, Aristotle University of Thessaloniki, 54124 Thessaloniki, Greece

Abstract—Integrated sensing and communication (ISAC) is seen as a future solution to frequency congestion due to its excellent ability to simultaneously support target sensing and information transmission. However, it also introduces a potential security threat due to the sensing behavior. In this paper, we propose a covert ISAC scheme against collusive wardens. In particular, a dual-function base station continuously sense an aerial target while communicating with a ground receiver. First, we derive a closed-form expression of each warden's detection outage probability to obtain the global detection outage probability. Then, we jointly optimize the communication and sensing beamformings to maximize the covert transmission rate under the worst case that all wardens can collusively adjust their detection thresholds to achieve the best detection. To tackle this non-convex optimization problem, an iteration scheme is proposed. Numerical results demonstrate the validity of the proposed covert ISAC scheme.

Index Terms—Integrated sensing and communication, covert communication, collusive detection.

I. INTRODUCTION

With the rapid development of mobile networks, the communication and radar devices are proliferating, putting tremendous pressure on the limited spectrum resource [1]. Integrated sensing and communication (ISAC) emerges as a promising technology to address this issue due to its particular ability to realize the communication and sensing services on a unified hardware platform simultaneously, and allow the communication and radar systems to share the same spectrum resource [2], [3]. Due to its high compatibility, ISAC can be combined with a variety of advanced techniques to improve performance, such as non-orthogonal multiple access [4], intelligent reflecting surface (IRS) [5], unmanned aerial vehicle [6], and so on. Nowadays, ISAC has been applied in various scenarios due to the above advantages, such as autonomous vehicle networks, smart home networks, and Internet of Things [7].

Recently, security issues have attracted considerable attention due to the inherent openness of wireless channels, which makes them highly susceptible to eavesdropping. To overcome this challenge, information encryption and physical layer security have been widely adopted in wireless networks to protect the transmitted information from being decrypted

Nan Zhao is the corresponding author (zhaonan@dlut.edu.cn). The work is supported by the National Natural Science Foundation of China (NSFC) under Grant U23A20271 and 62271099.

[8]. However, with the increasing security requirements, the transmission behavior should be hidden in some specific scenarios [9]. As a result, covert communication emerges to provide a higher level of security [10].

For ISAC, it is also threatened by unlawful interception, and how to design a covert ISAC has sparked a hot discussion [11]. At present, research on covert ISAC is in its infancy, and there are only a few initial works [11]-[14]. Ma et al. proposed a basic covert beamforming framework to maximize mutual information (MI) and covert rate in [11]. In [12], Hu et al. maximized the covert throughput while ensuring a high probability of radar sensing, thus achieving the tradeoff between radar sensing and covert transmission. Zhang et al. formulated an alternative optimization method for the IRS-aided covert ISAC to maximize the covert rate in [13]. However, the above works only focus on the case of a single warden, and the covert ISAC towards multiple wardens receives less attention. Ghosh et al. proposed a covert ISAC scheme with multiple wardens in [14], but the wardens can not cooperative with each other.

Motivated by these, we focus on the covert ISAC against collusive wardens. Specifically, the transmitter communicates with the legitimate user while sensing an aerial target, and the wardens are collusive to detect the legitimate transmission. First, we analyze each warden's detection performance and derive its optimal detection threshold to minimize the global detection outage probability. Then, we propose an iteration scheme to maximize the covert transmission rate via jointly optimizing the transmission and sensing beamformings.

Notation: $\Pr(A)$ is the probability of the occurrence of an event A. $\mathbb{E}(x)$, f(x) and $\mathcal{F}(x)$ are the expectation, the probability density function (PDF) and the cumulative distribution function (CDF) of a random variable x, respectively. $\Pr(\mathbf{S})$ and $\Pr(\mathbf{S})$ respectively denote the trace and rank of the square matrix \mathbf{S} .

II. SYSTEM MODEL

As shown in Fig. 1, we consider a covert ISAC network against randomly distributed Willies which are cooperate to detect. A dual-functional transmitter Alice with M antennas communicates with a single-antenna legitimate receiver Bob while keeping sensing an aerial target. In addition, a clustering-based detection is considered, where multiple

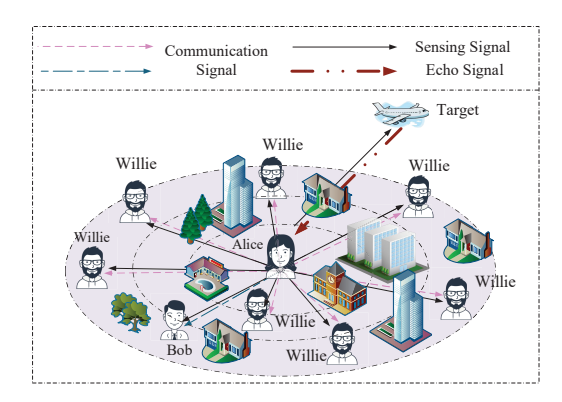


Fig. 1. Covert ISAC against randomly distributed collusive Willies.

single-antenna Willies collaborate with each other to monitor the communication. We employ a three-dimensional cylindrical coordinate system, where Alice, Bob and the target are located at $\mathcal{A}=(0\mathrm{m},0,0\mathrm{m}),\ \mathcal{B}=(r_b,\varphi_b,0\mathrm{m})$ and $\mathcal{G}=(r_t,\varphi_t,H)$, respectively. Assume that the T Willies are independently and uniformly distributed in a circular area with radius of D centered at Alice. The location of the t-th Willie is denoted as $\mathcal{W}_t(r_{wt},\varphi_{wt},0\mathrm{m}),t\in\mathcal{T},\mathcal{T}=\{1,2,\ldots,T\}$, which follows a binomial point process (BPP), i.e., $\mathcal{W}_t\sim\Phi_w$. The channel from Alice to Bob follows the large-scale path loss and Rayleigh fading, and the complex channel gain can be given as $\mathbf{g}_{ab}=\sqrt{\rho_0 r_{ab}^{-\alpha_g}}\mathbf{h}_{ab}\in\mathbb{C}^{M\times 1}$, where $\mathbf{h}_{ab}\sim\mathcal{CN}(\mathbf{0},\mathbf{I}_M)$ is modeled as complex Gaussian distributed, ρ_0 denotes the power gain at the reference distance of 1 m, α_g is the terrestrial path-loss exponent, and r_{ab} is the distance between Alice and Bob.

To sense the target, Alice consistently generates sensing signal and receives the echo. Assume that $x_s[i]$ is the deterministic sensing signal of the i-th channel use with $\mathbb{E}\left(|x_s[i]|^2\right)=1$, and $\mathbf{u}_s\in\mathbb{C}^{M\times 1}$ denotes the precoding vector for sensing, $i\in\mathcal{L},\mathcal{L}=\{1,2,\ldots,L\}$, where L is the number of available channel uses. Thus, the received signal at Bob with sensing signal can be expressed as

$$y_{B}[i] = \mathbf{g}_{ab}^{H} \mathbf{u}_{s} x_{s}[i] + n_{B}[i], i \in \mathcal{L},$$
(1)

where $n_{\rm B}[i] \sim \mathcal{CN}\left(0, \sigma_b^2\right)$ is the additive white Gaussian noise (AWGN) at Bob with the mean 0 and variance σ_b^2 .

When the communication and sensing signals are simultaneously transmitted, the received signal in the i-th channel use at Bob can be described as

$$y_{B}[i] = \mathbf{g}_{ab}^{H} \mathbf{u}_{s} x_{s}[i] + \mathbf{g}_{ab}^{H} \mathbf{u}_{c} x_{c}[i] + n_{B}[i], \qquad (2)$$

where $x_c[i]$ is the transmitted communication signal with $\mathbb{E}\left(|x_c[i]|^2\right)=1$, and Alice precodes the communication signal with the vector $\mathbf{u}_c\in\mathbb{C}^{M\times 1}$.

Accordingly, the signal-to-interference-plus-noise ratio (S-INR) at Bob γ_b can be obtained, and the transmission rate between Alice and Bob can be expressed as

$$R = \log_2\left(1 + \gamma_b\right) = \log_2\left(1 + \frac{|\mathbf{g}_{ab}^H \mathbf{u}_c|^2}{|\mathbf{g}_{ab}^H \mathbf{u}_s|^2 + \sigma_b^2}\right). \tag{3}$$

Without loss of generality, we consider to adopt the transmission rate in (3) subject to the covertness constraint as a measure of covert communication quality, which is also known as the covert transmission rate (CTR).

Similarly, the channel between Alice and the t-th Willie is also determined by both the large-scale path loss and small-scale Rayleigh fading, which can be modeled as $\mathbf{g}_{aw_t} = \sqrt{\rho_0 r_{aw_t}^{-\alpha_g}} \mathbf{h}_{aw_t} \in \mathbb{C}^{M \times 1}, t \in \mathcal{T}$, where $\mathbf{h}_{aw_t} \sim \mathcal{CN}(\mathbf{0}, \mathbf{I}_M)$, and r_{aw_t} denotes the distance between Alice and the t-th Willie. Therefore, the received signal in the i-th channel use at the t-th Willie with sensing signal can be expressed as

$$\mathbf{y}_{\mathbf{W}_{t}}[i] = \mathbf{g}_{aw_{t}}^{H} \mathbf{u}_{s} x_{s}[i] + n_{\mathbf{W}_{t}}[i], i \in \mathcal{L}, \tag{4}$$

where $n_{W_t}[i] \sim \mathcal{CN}\left(0, \sigma_{w_t}^2\right)$ denotes the AWGN at the t-th Willie. When the sensing and communication signals are both transmitted, the corresponding received signal at the t-th Willie can be represented as

$$\mathbf{y}_{\mathbf{W}_t}[i] = \mathbf{g}_{aw_t}^H \mathbf{u}_s x_s[i] + \mathbf{g}_{aw_t}^H \mathbf{u}_c x_c[i] + n_{\mathbf{W}_t}[i], i \in \mathcal{L}.$$
 (5)

Consider that the channel between Alice and aerial target is line-of-sight. In addition, due to the terrestrial environment, the echoes reflected from Bob and Willies can be negligible. Accordingly, the echo signal at Alice can be expressed as

$$y_{A}[i] = \Xi \mathbf{u}_{s} x_{s}[i] + \Xi \mathbf{u}_{c} x_{c}[i] + \mathbf{n}_{A}[i], \tag{6}$$

where $\Xi=\mu\mathbf{a}_T\mathbf{a}_R^H$, and μ is the complex amplitude related to the round-trip path-loss and the reflection factor of target. Moreover, \mathbf{a}_T and \mathbf{a}_R respectively denote the transmit steering vector and receive steering vector, which can be expressed as $\mathbf{a}_T=\mathbf{a}_R=\left[1,e^\psi,\ldots,e^{(M-1)\psi}\right]^T\in\mathbb{C}^{M\times 1}$ with $\psi=\frac{-j2\pi d\sin\phi}{\lambda}$, and ϕ represents the azimuth angle. Note that d denotes the spacing between the adjacent antennas, and λ denotes the carrier wavelength. In addition, $\mathbf{n}_A[i]\sim\mathcal{CN}(\mathbf{0},\sigma_a^2\mathbf{I}_M)$ denotes the AWGN at Alice.

Without loss of generality, MI is adopted to assess the quantity of information acquired by the transmitter from the echoes. Given $y_A[i]$ in (6), MI can be expressed as

$$I = \frac{1}{2} \log_2 \left(1 + \frac{\mathbf{u}_s^H \Xi^H \Xi \mathbf{u}_s}{\mathbf{u}_c^H \Xi^H \Xi \mathbf{u}_c + \sigma_a^2} \right). \tag{7}$$

It is demonstrated that increasing MI results in greater information acquisition of transmitter, consequently improving recognition capability [11]. To ensure sensing performance, we should guarantee that the MI is above a preset threshold.

III. DETECTION ANALYSIS AND OPTIMIZATION

Assume that Willies have full knowledge of CSI, as well as the prior transmission probability and transmit power, which creates the worst case for Alice. Besides, Willies can analyze the received power to determine whether Alice is transmitting. Therefore, the t-th Willie has to address a binary hypothesis testing as

(3)
$$\mathbf{y}_{\mathbf{W}_{t}}[i] = \begin{cases} \mathbf{g}_{aw_{t}}^{H} \mathbf{u}_{s} x_{s}[i] + n_{\mathbf{W}_{t}}[i], t \in \mathcal{T}, & \mathcal{H}_{0}, \\ \mathbf{g}_{aw_{t}}^{H} \mathbf{u}_{s} x_{s}[i] + \mathbf{g}_{aw_{t}}^{H} \mathbf{u}_{c} x_{c}[i] + n_{\mathbf{W}_{t}}[i], & \mathcal{H}_{1}, \end{cases}$$
(8)

where \mathcal{H}_0 is the null hypothesis suggesting that Alice does not engage in transmitting, while \mathcal{H}_1 is the alternative hypothesis proposing that Alice performs transmitting. Based on the average received power $\overline{P}_{w_t} = \left(\sum_{i=1}^L \left|\mathbf{y}_{\mathbf{W}_t[i]}\right|^2\right)/L$, the decision rule of the t-th Willie can be described as $\overline{P}_{w_t} \gtrsim \overline{\xi}_t$,

where $\overline{\xi}_t > 0$ is the t-th Willie's detection threshold. Considering $L \to \infty$, \overline{P}_{w_t} can be approximated as a stationary statistical random variable expressed as

$$P_{w_t} = \lim_{L \to \infty} \overline{P}_{w_t} = \begin{cases} S_{w_{tc}} + S_{w_{ts}} + \sigma_{w_t}^2, & \mathcal{H}_1, \\ S_{w_{ts}} + \sigma_{w_t}^2, & \mathcal{H}_0, \end{cases}$$
(9)

where $S_{wtc} = \rho_0 |\mathbf{h}_{aw_t}^H \mathbf{u}_c|^2 / r_{aw_t}^{\alpha_g}$ and $S_{wts} = \rho_0 |\mathbf{h}_{aw_t}^H \mathbf{u}_s|^2 / r_{aw_t}^{\alpha_g}$ are the average statistical powers of the sensing and communication, respectively.

Willies will inevitably make two kinds of errors during the detection, including the miss detection and false alarm. Based on the decision rule, the probability of the t-th Willie making a wrong detection can be given as

$$p_{w_{t}} = \Pr\{\mathcal{H}_{1}\} \Pr\{\mathcal{D}_{0} | \mathcal{H}_{1}\} + \Pr\{\mathcal{H}_{0}\} \Pr\{\mathcal{D}_{1} | \mathcal{H}_{0}\}$$

$$= \begin{cases} 0, & S_{w_{ts}} < \xi_{t} < S_{w_{tc}} + S_{w_{ts}}, \\ 0.5, & otherwise, \end{cases}$$
(10)

where $\xi_t = \overline{\xi}_t - \sigma_{w_t}^2$.

Without loss of generality, we define the probability that Willie makes error decision as detection outage probability (DOP), and the t-th Willie's DOP can be formulated as

$$p_{d_t} = 1 - \Pr\{p_{w_t} = 0\}$$

$$= 1 - \left(\mathcal{F}_{S_{w_{ts}}}(\xi_t) - \mathcal{F}_{S_{w_{ts}} + S_{w_{tc}}}(\xi_t)\right).$$
(11)

Due to $h_{a_m w_t} \sim \mathcal{CN}(0,1)$, $|\mathbf{h}_{aw_t} \mathbf{u}_c|^2$ and $|\mathbf{h}_{aw_t} \mathbf{u}_s|^2$ both follow an exponential distribution, indicating

$$S_{w_{tc}} \sim \exp\left(\frac{r_{aw_t}^{\alpha_g}}{\rho_0 P_{ac}}\right), \ S_{w_{ts}} \sim \exp\left(\frac{r_{aw_t}^{\alpha_g}}{\rho_0 P_{as}}\right),$$
 (12)

where $P_{as}\triangleq \|\mathbf{u}_s\|_2^2$ and $P_{ac}\triangleq \|\mathbf{u}_c\|_2^2$ denote the powers of sensing and communication, respectively. Thus, with $a_{tc}=r_{aw_t}^{\alpha_g}/(\rho_0P_{ac})$ and $a_{ts}=r_{aw_t}^{\alpha_g}/(\rho_0P_{as})$, the CDF of $S_{w_{ts}}$ can be calculated as $\mathcal{F}_{S_{w_{ts}}}(\xi_t)=1-e^{-a_{ts}\xi_t}$, and the CDF of $S_{w_{ts}}+S_{w_{tc}}$ can be calculated as

$$\mathcal{F}_{S_{w_{ts}}+S_{w_{tc}}}(\xi_{t}) = \int_{0}^{\xi_{t}} \int_{0}^{-x+\xi_{t}} a_{ts} e^{-a_{ts}x} a_{tc} e^{-a_{tc}y} dy dx$$

$$= \begin{cases} 1 - \frac{a_{tc}e^{a_{ts}} - a_{ts}e^{a_{tc}}}{(a_{tc} - a_{ts})e^{\xi_{t}}}, & a_{tc} \neq a_{ts}, \\ 1 - (1 + a_{tc}\xi_{t})e^{-a_{tc}\xi_{t}}, & a_{tc} = a_{ts}. \end{cases}$$
(13)

Therefore, the closed-form expression of p_{d_t} can be given as

$$P_{d_t} = \begin{cases} 1 - \frac{a_{ts} \left(e^{-a_{ts}\xi_t} - e^{-a_{tc}\xi_t} \right)}{a_{tc} - a_{ts}}, a_{tc} \neq a_{ts}, \\ 1 - a_{tc}\xi_t e^{-a_{tc}\xi_t}, a_{tc} = a_{ts}. \end{cases}$$
(14)

Willies collaborate on detecting the legitimate transmission with the covert transmission outage taking place when at least one Willie successfully detects it. With this context, the global DOP (GDOP) is defined to quantify the likelihood of all Willies failing to detect the transmission as

$$p_e = \mathbb{E}_{\Phi_w} \left[\Pr \left\{ \bigcap_{w_t \in \Phi_w} p_{w_t} \neq 0 \right\} \right] = \mathbb{E}_{\Phi_w} \left[\prod_{w_t \in \Phi_w} p_{d_t} \right]. \quad (15)$$

As Willies are independent and identically distributed and follow a BPP with PDF expressed as $f_{w_t}(r,\theta)=r/(\pi D^2)$, (15) can be calculated with $r_{aw_t}=r$ as

$$p_e = \prod_{t=1}^{T} \int_0^{2\pi} \int_0^D \frac{p_{d_t} r}{\pi D^2} dr d\theta = \left[\int_0^D \frac{2p_{d_t} r}{D^2} dr \right]^T.$$
 (16)

It is evident that the detection threshold significantly impacts the GDOP. Thus, each Willie aims to identify its own optimal detection threshold to minimize the GDOP. We derive the first-order derivative of p_e with respect to ξ_t defined as $p_{d_t}^{'}(\xi_t)$, and calculate the zero point of $p_{d_t}^{'}(\xi_t)$. Thus, the optimal detection threshold of each Willie can be detailed as

$$\xi_t^* = \begin{cases} \frac{\ln a_{ts} - \ln a_{tc}}{a_{ts} - a_{tc}}, a_{tc} \neq a_{ts}, \\ \frac{1}{a_{tc}}, a_{tc} = a_{ts}. \end{cases}$$
(17)

Adopting the optimal detection threshold in (17), the minimum DOP achieved by the t-th Willie can be calculated as

$$p_{d_t}^{\dagger} = \begin{cases} 1 - (a_{tc}/a_{ts})^{\frac{a_{tc}}{a_{ts} - a_{tc}}}, a_{tc} \neq a_{ts}, \\ 1 - e^{-1}, a_{tc} = a_{ts}, \end{cases}$$
(18)

accordingly, the optimal GDOP can be calculated as

$$p_e^{\dagger} = \begin{cases} \left(1 - (P_{as}/P_{ac})^{\frac{P_{as}}{P_{ac}-P_{as}}}\right)^T, P_{ac} \neq P_{as}, \\ \left(1 - e^{-1}\right)^T, P_{ac} = P_{as}. \end{cases}$$
(19)

When p_e^{\dagger} exceeds a specified threshold, the collaborative detection fails. It can be observed from (19) that the optimal GDOP is not related to M, indicating that increasing or decreasing the number of antennas have no impact on Willies' collaborative detection.

IV. CTR MAXIMIZATION

In this section, we jointly optimize the sensing vector \mathbf{u}_s and communication vector \mathbf{u}_c to maximize CTR while ensuring that MI remains above a preset threshold, with all Willies adopting the optimal detection thresholds.

A. Problem Formulation

The joint optimization problem can be formulated as

$$\mathbf{P1} : \max_{\mathbf{n} = \mathbf{n}} \quad R \tag{20a}$$

s.t.
$$I \ge \nu$$
, (20b)

$$p_e^{\dagger} > 1 - \varepsilon,$$
 (20c)

$$||\mathbf{u}_c||_2^2 \le P_{\text{cmax}},\tag{20d}$$

$$||\mathbf{u}_s||_2^2 \le P_{\text{smax}}.$$
 (20e)

Note that (20b) serves as the MI constraint to guarantee the sensing performance, and $1-\varepsilon$ in (20c) is the minimum required GDOP with ε denoting the covertness level. $P_{\rm smax}$ and $P_{\rm cmax}$ represent the maximum available sensing and transmission powers, respectively.

Due to the highly coupled vectors, and non-convex objective function and constraints, it is difficult to solve P1. To address this challenge, P1 can be converted into a standard semi-definite programming.

The channels can be reformulated as $\mathbf{G}_{ab} = \mathbf{g}_{ab}\mathbf{g}_{ab}^H$ and $\mathbf{G}_T = \mathbf{a}_T\mathbf{a}_T^H$. The Hermitian matrices of \mathbf{u}_s and \mathbf{u}_c can also be obtained as $\mathbf{U}_c = \mathbf{u}_c\mathbf{u}_c^H$ and $\mathbf{U}_s = \mathbf{u}_s\mathbf{u}_s^H$ satisfying

$$\mathbf{U}_c \succeq 0, \mathbf{U}_s \succeq 0, \operatorname{Ra}(\mathbf{U}_c) = \operatorname{Ra}(\mathbf{U}_s) = 1.$$
 (21)

Moreover, P_{ac} and P_{as} can be expressed as

$$P_{ac} = \text{Tr}(\mathbf{U}_c), P_{as} = \text{Tr}(\mathbf{U}_s). \tag{22}$$

According to the above transformation, P1 can be recast as

$$\mathbf{P2}: \max_{\mathbf{U}_s, \mathbf{U}_c} \quad R \tag{23a}$$

s.t.
$$(20b)$$
, $(20c)$ and (21) , $(23b)$

$$Tr(\mathbf{U}_c) \le P_{cmax},$$
 (23c)

$$\operatorname{Tr}(\mathbf{U}_s) \le P_{\operatorname{smax}}.$$
 (23d)

Due to the complex expression of CTR, we can rewrite R at the top on the next page in (24), which is a concaveminus-concave expression. Thus, a global upper estimator of the concave expression $\widehat{R}(\mathbf{U}_s)$ can be afforded via the first-order Taylor expansion, which can be described with a given local point as

$$\widehat{R}(\mathbf{U}_s) \leq \widehat{R}^{[lp]}(\mathbf{U}_s) = \widehat{R}\left(\mathbf{U}_s^{(p)}\right) + \operatorname{Tr}\left(\nabla_{\mathbf{U}_s^{(p)}}^H \widehat{R}\left(\mathbf{U}_s^{(p)}\right) \left(\mathbf{U}_s - \mathbf{U}_s^{(p)}\right)\right),$$
(25)

where p denotes the iteration index, and $\mathbf{U}_s^{(p)}$ represent the optimized \mathbf{U}_s in the p-th iteration. Note that $\widehat{R}(\mathbf{U}_s^{(p)})$ can be calculated by substituting $\mathbf{U}_s^{(p)}$ into (24) as

$$\widehat{R}\left(\mathbf{U}_{s}^{(p)}\right) = \log_{2}\left(\operatorname{Tr}\left(\mathbf{G}_{ab}\mathbf{U}_{s}^{(p)}\right) + \sigma_{b}^{2}\right).$$
 (26)

In addition, $\bigtriangledown_{\mathbf{U}_{s}^{(p)}}^{H}\widehat{R}\left(\mathbf{U}_{s}^{(p)}\right)$ can be given by

$$\nabla_{\mathbf{U}_{s}^{(p)}}^{H}\widehat{R}\left(\mathbf{U}_{s}^{(p)}\right) = -\frac{1}{\ln 2} \frac{\mathbf{G}_{ab}}{\operatorname{Tr}\left(\mathbf{G}_{ab}\mathbf{U}_{s}^{(p)}\right) + \sigma_{b}^{2}}.$$
 (27)

Thus, (23a) can be transformed into

$$\max_{\mathbf{U}_s, \mathbf{U}_c} \quad \widetilde{R} - \widehat{R}^{[lp]}(\mathbf{U}_s). \tag{28}$$

Moreover, (20b) can be converted as

$$|\mu|^{2} \operatorname{Tr}(\mathbf{G}_{T} \mathbf{U}_{s}) \ge (2^{\nu} - 1) \left(|\mu|^{2} \operatorname{Tr}(\mathbf{G}_{T} \mathbf{U}_{c}) + \sigma_{a}^{2} / \operatorname{Tr}(\mathbf{G}_{T}) \right).$$
(29)

which is convex.

For (20c), because of the complex expression of p_e^{\dagger} , it

is difficult to judge whether (20c) is convex. Thus, we first rewrite it as

$$1 - (P_{as}/P_{ac})^{\frac{P_{as}}{P_{ac} - P_{as}}} \ge \sqrt[T]{1 - \varepsilon},\tag{30}$$

which can be simplified as

$$(P_{as}/P_{ac})^{\frac{P_{as}}{P_{ac}-P_{as}}} + \vartheta \le 0, \vartheta = \sqrt[T]{1-\varepsilon} - 1 < 0.$$
 (31)

To handle the exponential function, the logarithmic function is introduced to transform (31) into

$$\frac{P_{as}}{P_{as} - P_{ac}} \ln \left(\frac{P_{as}}{P_{ac}}\right) + \ln \left(-\vartheta\right) \ge 0. \tag{32}$$

Unfortunately, it is still difficult to determine whether $\frac{P_{as}}{P_{as}-P_{ac}}\ln(\frac{P_{as}}{P_{ac}})$ is a convex or concave function. Therefore, we will solve the problem in two classifications, i.e., $P_{as}-P_{ac}>0$ and $P_{as}-P_{ac}<0$.

1)
$$P_{as} - P_{ac} > 0$$
:

With $P_{as} - P_{ac} > 0$, (32) can be transformed as

$$P_{as} \ln (P_{as}/P_{ac}) + (P_{as} - P_{ac}) \ln (-\vartheta) \ge 0.$$
 (33)

For convenience, we define $f(P_{as}; P_{ac}) = P_{as} \ln{(P_{as}/P_{ac})}$, and the Hessian Matrix of $f(P_{as}; P_{ac})$ can be calculated as

$$\nabla^2 f(P_{as}; P_{ac}) = \begin{bmatrix} \frac{1}{P_{as}} & -\frac{1}{P_{ac}} \\ -\frac{1}{P_{ac}} & \frac{P_{as}}{P_{ac}^2} \end{bmatrix} \succeq 0.$$
 (34)

According to (34), we can conclude that $\nabla^2 f(P_{as}; P_{ac})$ is a positive semi-definite matrix, indicating that $f(P_{as}; P_{ac})$ is convex. However, it is obvious that $(P_{as} - P_{ac}) \ln{(-\vartheta)}$ is linear, and (33) is convex-plus-linear, which is not convex. Thus, we can similarly approximate $f(P_{as}; P_{ac})$ via the first-order Taylor expansion described as (35) at the top of next page. In the same way, p denotes the iteration index, and $P_{as}^{(p)} = \text{Tr}(\mathbf{U}_{s}^{(p)}), P_{ac}^{(p)} = \text{Tr}(\mathbf{U}_{c}^{(p)})$ represent the optimized communication and sensing powers in the p-th iteration.

Based on the above conversion, (33) can eventually be transformed as

$$\widehat{f}(\operatorname{Tr}(\mathbf{U}_s); \operatorname{Tr}(\mathbf{U}_c)) + (\operatorname{Tr}(\mathbf{U}_s) - \operatorname{Tr}(\mathbf{U}_c)) \ln(-\vartheta) \ge 0.$$
 (36)

2) $P_{as} - P_{ac} < 0$:

Similarly, with $P_{as} - P_{ac} < 0$, (32) be converted as

$$f(P_{as}; P_{ac}) + (P_{as} - P_{ac}) \ln(-\vartheta) \le 0,$$
 (37)

which is a convex constraint, and can be rewritten as

$$f(\operatorname{Tr}(\mathbf{U}_s); \operatorname{Tr}(\mathbf{U}_c)) + (\operatorname{Tr}(\mathbf{U}_s) - \operatorname{Tr}(\mathbf{U}_c)) \ln(-\vartheta) \le 0.$$
 (38)

Henceforth, all the constraints are transformed into convex ones except for the rank-1 constraint, which can be relaxed to tackle the non-convex obstacle. Based on the above transformation, **P2** can be converted as

$$\mathbf{P3.1}: \max_{\mathbf{U}_s \succeq 0, \mathbf{U}_c \succeq 0} \qquad \widetilde{R} - \widehat{R}^{[lp]}(\mathbf{U}_s)$$
 (39a)

s.t.
$$(23c), (23d), (29), (36)$$
 (39b)

$$Tr(\mathbf{U}_s - \mathbf{U}_c) > 0, \tag{39c}$$

$$R = \log_2\left(1 + \frac{\operatorname{Tr}\left(\mathbf{G}_{ab}\mathbf{U}_c\right)}{\operatorname{Tr}\left(\mathbf{G}_{ab}\mathbf{U}_s\right) + \sigma_b^2}\right) = \log_2\left(\operatorname{Tr}\left(\mathbf{G}_{ab}\left(\mathbf{U}_c + \mathbf{U}_s\right)\right) + \sigma_b^2\right) - \log_2\left(\operatorname{Tr}\left(\mathbf{G}_{ab}\mathbf{U}_s\right) + \sigma_b^2\right) \triangleq \widetilde{R} - \widehat{R}\left(\mathbf{U}_s\right). \quad (24)$$

$$f(P_{as}; P_{ac}) \ge f(P_{as}^{(p)}; P_{ac}^{(p)}) + \left(\ln \frac{P_{as}^{(p)}}{P_{ac}^{(p)}} + 1\right) \left(P_{as} - P_{as}^{(p)}\right) - \frac{P_{as}^{(p)}}{P_{ac}^{(p)}} \left(P_{ac} - P_{ac}^{(p)}\right) \triangleq \widehat{f}(P_{as}; P_{ac}). \tag{35}$$

and

$$\mathbf{P3.2}: \max_{\mathbf{U}_s \succeq 0, \mathbf{U}_c \succeq 0} \qquad \widetilde{R} - \widehat{R}^{[lp]}(\mathbf{U}_s)$$
 (40a)

s.t.
$$(23c), (23d), (29), (38)$$
 (40b)

$$Tr(\mathbf{U}_s - \mathbf{U}_c) < 0, \tag{40c}$$

which are both convex, and can be tackled via a standard convex optimization solver such as CVX. Due to the relaxation of rank-1 constraint, $Ra(\mathbf{U}_c^*) = Ra(\mathbf{U}_s^*) = 1$ may not be satisfied. Gaussian randomization process can be adopted to address the issue to attain a high-quality rank-1 solution.

With the identical channels, solving P3.1 and P3.2 can yield their own optimal solutions, and we can obtain the final solution to P2 by comparing the optimal CTR achieved by the two sets of optimal solutions. The specific steps are detailed in Algorithm 1, where ς is the convergence estimation sign.

Algorithm 1 - the iteration for (23)

- 1: **Initialization**: Initialize $\mathbf{u}_s^{(0)},~\mathbf{u}_c^{(0)}$ and ς , and set the iteration index l=0, a=0. Calculate $R^{(0)}$ with the initial settings.
- 2: repeat
- Update: l = l + 1.
- Optimize the beamforming vectors via (39).
- 5: **until** $R^{(l)} R^{(l-1)} < \varsigma$.
- Update: a = a + 1. 7:
- Optimize the beamforming vectors via (40).
- 9: **until** $R^{(a)} R^{(a-1)} \le \varsigma$.
- 10: If $R^{(l)} > R^{(a)}$, $R^* = R^{(l)}$, $\mathbf{u}_s^* = \mathbf{u}_s^{(l)}$ and $\mathbf{u}_c^* = \mathbf{u}_c^{(l)}$. 11: If $R^{(l)} < R^{(a)}$, $R^* = R^{(a)}$, $\mathbf{u}_s^* = \mathbf{u}_s^{(a)}$ and $\mathbf{u}_c^* = \mathbf{u}_c^{(a)}$.
- 12: Output: \mathbf{u}_{s}^{*} , \mathbf{u}_{c}^{*} and R^{*} .

V. SIMULATION RESULTS

In this section, we evaluate the performance of the proposed covert ISAC scheme through simulation results. Unless explicitly specified, the relevant parameters are set according to the following defaults. Alice, Bob and the target are located at A = (0m, 0, 0m), $B = (50m, \frac{\pi}{4}, 0m)$ and $\mathcal{G} = (60 \text{m}, \frac{3\pi}{4}, 150 \text{m})$, respectively. The radius is set as D=300 m. The number of antennas equipped at Alice is M=8, and the number of Willies is T=5. Without loss of generality, the spacing between two adjacent antennas is assumed to be $d = 0.5\lambda$, and the azimuth angle is given as

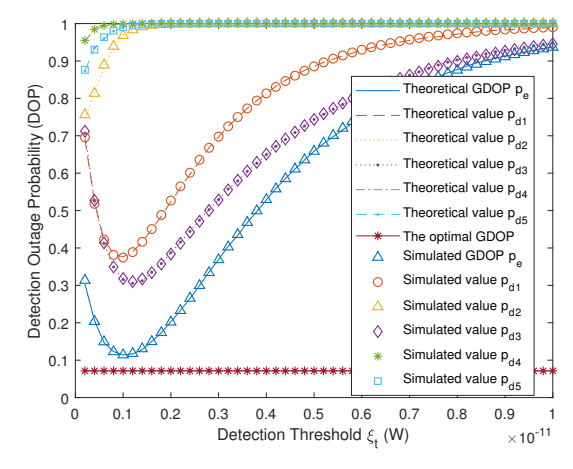


Fig. 2. Comparison of the DOP and GDOP under different detection

 $\phi = \frac{\pi}{3}$. In addition, the air-to-ground and terrestrial pathloss exponents are set as $\alpha_s = 2$ and $\alpha_g = 2.8$, respectively. The path-loss gain at the reference distance is established as $ho_0=-40$ dB. Moreover, the noise power at Alice, Bob and the t-th Willie can be assumed as $\sigma_a^2=\sigma_b^2=\sigma_{w_t}^2=-110$ dB, and the covertness level is $\varepsilon = 0.1$.

The theoretical and simulated DOP p_{dt} and GDOP p_e with respect to the detection threshold ξ_t are presented in Fig. 2 with $P_{as} = 30$ mW and $P_{ac} = 10$ mW. In addition, the optimal GDOP is also displayed in Fig. 2 with Willies' optimal detection thresholds. First, we can observe that the theoretical and simulated values of DOP and GDOP can fit perfectly, proving the derivation in Section III. Moreover, the DOP varies with ξ_t , and there exist different optimal detection thresholds for Willies to minimize the DOP. Furthermore, the GDOP is smaller than any DOP, indicating that Willies' cooperation is effective. As each Willie adopts the optimal detection threshold, we can find that the optimal GDOP is smallest that improves the detection performance effectively.

Fig. 3 portrays the impacts of sensing and communication powers on GDOP with different number of Willies T. First, it can be observed that the GDOP decreases monotonically with increasing T, and a larger T leads to a much lower GDOP, suggesting that the choice of T should be based on a comprehensive consideration of both GDOP and detection efficiency. Furthermore, we observe that GDOP decreases as P_{ac} increases, which is due to the fact that higher P_{ac} results in greater received power at each Willie, thereby improving the correctness of its binary hypothesis testing. In contrast, the GDOP increases as P_{as} increases, due to the fact that

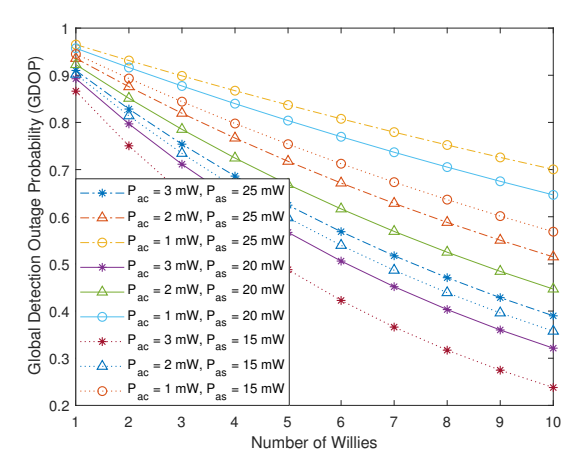


Fig. 3. Comparison of the influence of communication power P_{ac} and sensing power P_{as} on GDOP with different number of Willies.

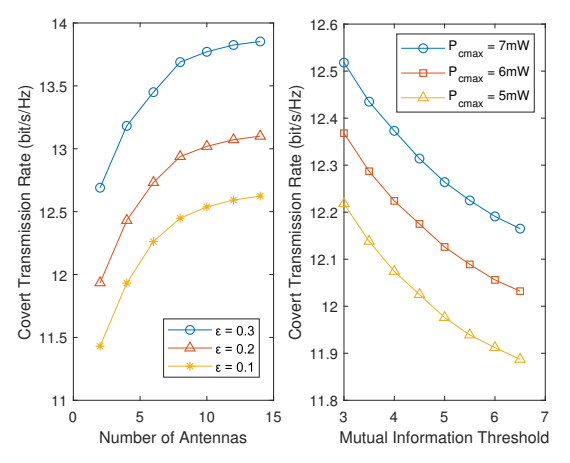


Fig. 4. Covert transmission rate versus different number of antennas and mutual information thresholds.

the sensing signal is seen as interference to the Willies. Increasing P_{as} leads to more uncertainty for Willies, and consequently decreases detection performance.

We further investigate the influence of number of antennas on CTR in Fig. 4 with $P_{\rm cmax}=5$ mW and $P_{\rm smax}=20$ mW, where $\varepsilon=0.1,\, \varepsilon=0.2$ and $\varepsilon=0.3$ are considered. It can be observed that the CTR increases with M, however, this trend tends to be slow. The results remind us that although increasing M does not pose an additional threat to the covert communication while increasing the transmission rate, it is essential to take into account the transmission efficiency in practical scenarios. In addition, the covertness and CTR should be traded off, and the improvement of covertness can inevitably lead to the decrease of communication performance, and vice versa. The CTR increases with ε , because an increase in ε indicates that the requirement of covertness is relaxed, thus, Alice can appropriately increase P_{ac} to improve the communication quality. Moreover, we also study the impact of MI threshold on CTR in Fig. 4. As can be observed, the MI and CTR are a pair of metrics that constrain each other, which can not be both enhanced. The CTR decreases with increasing MI threshold, which can be attributed to that the communication signal is considered as interference during the sensing. Consequently, as the threshold becomes more stringent, Alice has to lower P_{ac} to satisfy the sensing requirement, resulting in a detrimental effect on the CTR.

VI. CONCLUSIONS

In this paper, we have investigated the covert ISAC of a dual-functional transmitter towards collusive wardens. MI and CTR are adopted as the metrics of sensing and communication, respectively. The detection performance of each Willie is analyzed and the optimal detection thresholds are derived to achieve the minimal GDOP. Under this worst situation, we jointly optimize the communication and sensing beamformings to maximize the CTR while ensuring the covertness and effective sensing. Hence, a non-convex optimization problem is formulated, and a scheme applying first-order Taylor expansion is leveraged to address it. Simulation results demonstrate that the proposed scheme can achieve the trade-off among the covertness, communication and sensing.

REFERENCES

- X. You et al., "Towards 6G wireless communication networks: vision, enabling technologies, and new paradigm shifts," Sci. China Inf. Sci., vol. 64, art. no. 110301, 2021.
- [2] F. Liu, L. Zheng, Y. Cui, C. Masouros, A. P. Petropulu, H. Griffiths, and Y. C. Eldar, "Seventy years of radar and communications: The road from separation to integration," *IEEE Signal Process Mag.*, vol. 40, no. 5, pp. 106–121, Jul. 2023.
- [3] J. Zhang, W. Lu, C. Xing, N. Zhao, N. Al-Dhahir, G. K. Karagiannidis, and X. Yang, "Intelligent integrated sensing and communication: a survey," Sci. China Inf. Sci., vol. 68, no. 3, p. Art. no. 131301, Mar. 2025.
- [4] X. Mu, Y. Liu, L. Guo, J. Lin, and L. Hanzo, "NOMA-aided joint radar and multicast-unicast communication systems," *IEEE J. Sel. Areas Commun.*, vol. 40, no. 6, pp. 1978–1992, Jun. 2022.
- [5] M. Shi, X. Li, J. Liu, and S. Lv, "Constant modulus waveform design for RIS-aided ISAC system," *IEEE Trans. Veh. Technol.*, vol. 73, no. 6, pp. 8648–8659, Jun. 2024.
- [6] Z. Lyu, G. Zhu, and J. Xu, "Joint maneuver and beamforming design for UAV-enabled integrated sensing and communication," *IEEE Trans. Wireless Commun.*, vol. 22, no. 4, pp. 2424–2440, Apr. 2023.
- [7] F. Liu, Y. Cui, C. Masouros, J. Xu, T. X. Han, Y. C. Eldar, and S. Buzzi, "Integrated sensing and communications: Toward dualfunctional wireless networks for 6G and beyond," *IEEE J. Sel. Areas Commun.*, vol. 40, pp. 1728–1767, Jun. 2022.
- [8] Y. Zou, J. Zhu, X. Wang, and L. Hanzo, "A survey on wireless security: Technical challenges, recent advances, and future trends," *Proc. IEEE*, vol. 104, no. 9, pp. 1727–1765, Sept. 2016.
- [9] X. Chen, J. An, Z. Xiong, C. Xing, N. Zhao, F. R. Yu, and A. Nallanathan, "Covert communications: A comprehensive survey," *IEEE Commun. Surv. Tut.*, vol. 25, no. 2, pp. 1173–1198, 2nd Quart. 2023.
- [10] B. A. Bash, D. Goeckel, D. Towsley, and S. Guha, "Hiding information in noise: Fundamental limits of covert wireless communication," *IEEE Commun. Mag.*, vol. 53, no. 12, pp. 26–31, Dec. 2015.
- [11] S. Ma, H. Sheng, R. Yang, H. Li, Y. Wu, C. Shen, N. Al-Dhahir, and S. Li, "Covert beamforming design for integrated radar sensing and communication systems," *IEEE Trans. Wireless Commun.*, vol. 22, no. 1, pp. 718–731, Jan. 2023.
- [12] J. Hu, Q. Lin, S. Yan, X. Zhou, Y. Chen, and F. Shu, "Covert transmission via integrated sensing and communication systems," *IEEE Trans. Veh. Technol.*, vol. 73, no. 3, pp. 4441–4446, Mar. 2024.
- [13] Y. Zhang, W. Ni, J. Wang, W. Tang, M. Jia, Y. C. Eldar, and D. Niyato, "Robust transceiver design for covert integrated sensing and communications with imperfect CSI," *IEEE Trans. Commun.*, to appear.
- [14] I. Ghosh, A. Chattopadhyay, K. V. Mishra, and A. P. Petropulu, "Multicast with multiple wardens in IRS-aided covert DFRC system," in *Proc. IEEE ICASSP'24*, pp. 12871–12875, Seoul, Korea, Apr. 2024.